

Cooperative gas adsorption without a phase transition in metal-organic frameworks

J. F. Stilck

Instituto de Física and INCT-SC, UFF
Niterói.

COLMEA-UFF, 20/6/2018

Outline

- 1 Introduction
- 2 Model and transfer matrix solution
- 3 Comparison with experiments
- 4 Conclusion and outlook

Outline

- 1 Introduction
- 2 Model and transfer matrix solution
- 3 Comparison with experiments
- 4 Conclusion and outlook

Outline

- 1 Introduction
- 2 Model and transfer matrix solution
- 3 Comparison with experiments
- 4 Conclusion and outlook

Outline

- 1 Introduction
- 2 Model and transfer matrix solution
- 3 Comparison with experiments
- 4 Conclusion and outlook

Collaborators

Work done in collaboration with Joyjit Kundu^{1,2}, Jung-Hoon Lee^{1,3}, Jeffrey B. Neaton^{1,3,4}, David Prendergast¹, and Stephen Whitelam¹.

1-Molecular Foundry, Lawrence Berkeley National Laboratory.

2-Department of Chemistry, Duke University, Durham.

3-Department of Physics, University of California, Berkeley.

4-Kavli Energy Nanosciences Institute at Berkeley, Berkeley.

(paper at <https://arxiv.org/abs/1712.05061>)



D. Dhar.



R. Rajesh.



J. Kundu.

CO₂ adsorption

- Technology for CO₂ capture and storage: Metal-organic frameworks (MOF's). Porous materials, tunable molecular properties, large internal surface area.
- Most MOF's: Langmuir type isotherms. Small number of MOF's: step-like adsorption isotherms, more convenient from technological point of view.
- Usually this is attributed to first-order phase transition or a dynamic rearrangement of the framework.
- In some diamine-appended MOF's, (*mmen* – M₂, where M stands for the metal Mg, Mn, Fe, Co, or Zn), no evidence for either, origin of cooperativity unclear.
- Experimental measurements and DFT calculations: at higher partial pressures CO₂ undergoes chemisorption, forming ammonium carbamate chains along the c-axis of MOF.

CO₂ adsorption

- Technology for CO₂ capture and storage: Metal-organic frameworks (MOF's). Porous materials, tunable molecular properties, large internal surface area.
- Most MOF's: Langmuir type isotherms. Small number of MOF's: step-like adsorption isotherms, more convenient from technological point of view.
- Usually this is attributed to first-order phase transition or a dynamic rearrangement of the framework.
- In some diamine-appended MOF's, (*mmen* – M₂, where M stands for the metal Mg, Mn, Fe, Co, or Zn), no evidence for either, origin of cooperativity unclear.
- Experimental measurements and DFT calculations: at higher partial pressures CO₂ undergoes chemisorption, forming ammonium carbamate chains along the c-axis of MOF.

CO₂ adsorption

- Technology for CO₂ capture and storage: Metal-organic frameworks (MOF's). Porous materials, tunable molecular properties, large internal surface area.
- Most MOF's: Langmuir type isotherms. Small number of MOF's: step-like adsorption isotherms, more convenient from technological point of view.
- Usually this is attributed to first-order phase transition or a dynamic rearrangement of the framework.
- In some diamine-appended MOF's, (*mmen* – M₂, where M stands for the metal Mg, Mn, Fe, Co, or Zn), no evidence for either, origin of cooperativity unclear.
- Experimental measurements and DFT calculations: at higher partial pressures CO₂ undergoes chemisorption, forming ammonium carbamate chains along the c-axis of MOF.

CO₂ adsorption

- Technology for CO₂ capture and storage: Metal-organic frameworks (MOF's). Porous materials, tunable molecular properties, large internal surface area.
- Most MOF's: Langmuir type isotherms. Small number of MOF's: step-like adsorption isotherms, more convenient from technological point of view.
- Usually this is attributed to first-order phase transition or a dynamic rearrangement of the framework.
- In some diamine-appended MOF's, (*mmen* – M₂, where M stands for the metal Mg, Mn, Fe, Co, or Zn), no evidence for either, origin of cooperativity unclear.
- Experimental measurements and DFT calculations: at higher partial pressures CO₂ undergoes chemisorption, forming ammonium carbamate chains along the c-axis of MOF.

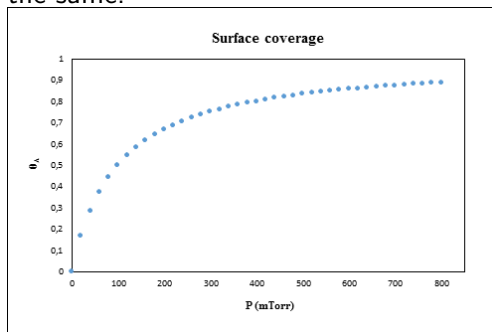
CO₂ adsorption

- Technology for CO₂ capture and storage: Metal-organic frameworks (MOF's). Porous materials, tunable molecular properties, large internal surface area.
- Most MOF's: Langmuir type isotherms. Small number of MOF's: step-like adsorption isotherms, more convenient from technological point of view.
- Usually this is attributed to first-order phase transition or a dynamic rearrangement of the framework.
- In some diamine-appended MOF's, (*mmen* – M₂, where M stands for the metal Mg, Mn, Fe, Co, or Zn), no evidence for either, origin of cooperativity unclear.
- Experimental measurements and DFT calculations: at higher partial pressures CO₂ undergoes chemisorption, forming ammonium carbamate chains along the c-axis of MOF.

CO₂ adsorption

Langmuir adsorption (1918): monomers are adsorbed on substrate, at most one at each site (monolayer). Gas in bulk is ideal.

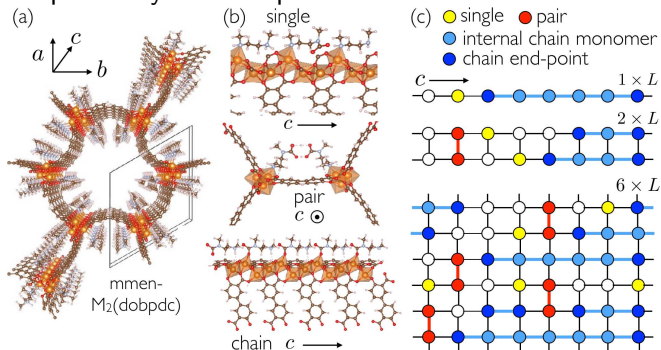
Equilibrium: chemical potentials in bulk and adsorbed phase are the same.



$$\Theta_A = \frac{P}{P + P_0(T)}. \text{ Data generated for } P_0 = 100 \text{ mTorr}$$

Model

Mapping of system on one dimensional exactly solvable statistical-mechanical model, parametrized by DFT calculations: cooperativity without phase transition.



Equilibrium polymerization model

- P. M. Pfeuty and J. C. Wheeler, Phys. Rev. A **27**, 2178 (1983): equilibrium polymerization in one dimension (polymerization of liquid sulfur). 1-lane model.
- Grand-canonical partition function:

$$\mathcal{Z} = \sum_{\{n_1, n_i, n_e\}} K_1^{n_1} K_e^{n_e} K_i^{n_i} \Gamma(n_1, n_i, n_e).$$

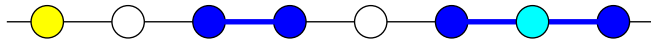
Equilibrium polymerization model

- P. M. Pfeuty and J. C. Wheeler, Phys. Rev. A **27**, 2178 (1983): equilibrium polymerization in one dimension (polymerization of liquid sulfur). 1-lane model.
- Grand-canonical partition function:

$$\mathcal{Z} = \sum_{\{n_1, n_i, n_e\}} K_1^{n_1} K_e^{n_e} K_i^{n_i} \Gamma(n_1, n_i, n_e).$$

Equilibrium polymerization model

Portion of lattice in a particular configuration and associated statistical weight:



$$\mathbf{K}_1 \mathbf{K}_e^4 \mathbf{K}_i$$

Equilibrium polymerization model

- Edges: with ($\eta = 1$) or without ($\eta = 0$) bond on them.
- Transfer matrix elements: $T_{00} = 1 + K_1$, $T_{01} = T_{10} = K_e$,
 $T_{11} = K_i$.
- 2×2 transfer matrix:

$$T = \begin{pmatrix} 1 + K_1 & K_e \\ K_e & K_i \end{pmatrix}.$$

- Perron-Frobenius theorem: no phase transition for $K_e \neq 0$.
- When $K_e, K_i = 0$ (no chains): Langmuir.

Equilibrium polymerization model

- Edges: with ($\eta = 1$) or without ($\eta = 0$) bond on them.
- Transfer matrix elements: $T_{00} = 1 + K_1$, $T_{01} = T_{10} = K_e$,
 $T_{11} = K_i$.
- 2×2 transfer matrix:

$$T = \begin{pmatrix} 1 + K_1 & K_e \\ K_e & K_i \end{pmatrix}.$$

- Perron-Frobenius theorem: no phase transition for $K_e \neq 0$.
- When $K_e, K_i = 0$ (no chains): Langmuir.

Equilibrium polymerization model

- Edges: with ($\eta = 1$) or without ($\eta = 0$) bond on them.
- Transfer matrix elements: $T_{00} = 1 + K_1$, $T_{01} = T_{10} = K_e$,
 $T_{11} = K_i$.
- 2×2 transfer matrix:

$$T = \begin{pmatrix} 1 + K_1 & K_e \\ K_e & K_i \end{pmatrix}.$$

- Perron-Frobenius theorem: no phase transition for $K_e \neq 0$.
- When $K_e, K_i = 0$ (no chains): Langmuir.

Equilibrium polymerization model

- Edges: with ($\eta = 1$) or without ($\eta = 0$) bond on them.
- Transfer matrix elements: $T_{00} = 1 + K_1$, $T_{01} = T_{10} = K_e$,
 $T_{11} = K_i$.
- 2×2 transfer matrix:

$$T = \begin{pmatrix} 1 + K_1 & K_e \\ K_e & K_i \end{pmatrix}.$$

- Perron-Frobenius theorem: no phase transition for $K_e \neq 0$.
- When $K_e, K_i = 0$ (no chains): Langmuir.

Equilibrium polymerization model

- Edges: with ($\eta = 1$) or without ($\eta = 0$) bond on them.
- Transfer matrix elements: $T_{00} = 1 + K_1$, $T_{01} = T_{10} = K_e$,
 $T_{11} = K_i$.
- 2×2 transfer matrix:

$$T = \begin{pmatrix} 1 + K_1 & K_e \\ K_e & K_i \end{pmatrix}.$$

- Perron-Frobenius theorem: no phase transition for $K_e \neq 0$.
- When $K_e, K_i = 0$ (no chains): Langmuir.

Equilibrium polymerization model

- Eigenvalues of transfer matrix:

$$2\lambda_{\pm} = 1 + K_1 + K_i \pm \sqrt{(1 + K_1 - K_i)^2 + 4K_e^2}.$$

- Free energy per site: $f = -k_B T \ln \lambda_+$. Phase transition only in the limit $K_e = 0$.
- In this limit, $\Theta_{A,1} = K_1/(1 + K_1)$, $\Theta_{A,i} = 0$, for $1 + K_1 > K_i$.
- $\Theta_{A,1} = 0$, $\Theta_{A,i} = 1$, for $1 + K_1 < K_i$.

Equilibrium polymerization model

- Eigenvalues of transfer matrix:

$$2\lambda_{\pm} = 1 + K_1 + K_i \pm \sqrt{(1 + K_1 - K_i)^2 + 4K_e^2}.$$

- Free energy per site: $f = -k_B T \ln \lambda_+$. Phase transition only in the limit $K_e = 0$.
- In this limit, $\Theta_{A,1} = K_1/(1 + K_1)$, $\Theta_{A,i} = 0$, for $1 + K_1 > K_i$.
- $\Theta_{A,1} = 0$, $\Theta_{A,i} = 1$, for $1 + K_1 < K_i$.

Equilibrium polymerization model

- Eigenvalues of transfer matrix:

$$2\lambda_{\pm} = 1 + K_1 + K_i \pm \sqrt{(1 + K_1 - K_i)^2 + 4K_e^2}.$$

- Free energy per site: $f = -k_B T \ln \lambda_+$. Phase transition only in the limit $K_e = 0$.
- In this limit, $\Theta_{A,1} = K_1/(1 + K_1)$, $\Theta_{A,i} = 0$, for $1 + K_1 > K_i$.
- $\Theta_{A,1} = 0$, $\Theta_{A,i} = 1$, for $1 + K_1 < K_i$.

Equilibrium polymerization model

- Eigenvalues of transfer matrix:

$$2\lambda_{\pm} = 1 + K_1 + K_i \pm \sqrt{(1 + K_1 - K_i)^2 + 4K_e^2}.$$

- Free energy per site: $f = -k_B T \ln \lambda_+$. Phase transition only in the limit $K_e = 0$.
- In this limit, $\Theta_{A,1} = K_1/(1 + K_1)$, $\Theta_{A,i} = 0$, for $1 + K_1 > K_i$.
- $\Theta_{A,1} = 0$, $\Theta_{A,i} = 1$, for $1 + K_1 < K_i$.

Equilibrium polymerization model

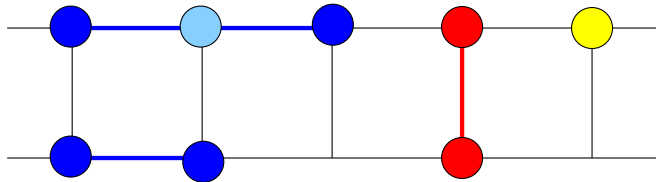
- Drawback: independent lanes since no transverse bonding (dimers) are present.
- To include dimers: 2-lane (still exactly solvable, 4×4 transfer matrix) and 6-lane model (64×64 transfer matrix).

Equilibrium polymerization model

- Drawback: independent lanes since no transverse bonding (dimers) are present.
- To include dimers: 2-lane (still exactly solvable, 4×4 transfer matrix) and 6-lane model (64×64 transfer matrix).

Equilibrium polymerization model

Two-lane model. Portion of the lattice and statistical weight:



$$\mathbf{K}_1 \mathbf{K}_e^4 \mathbf{K}_i \mathbf{K}_d$$

Examples of transfer matrix element: $T_{00,00} = (1 + K_1)^2 + K_d$;

$T_{10,00} = K_e(1 + K_1)$.

Equilibrium polymerization model

The chemical equilibrium constants K_α , $\alpha = 1, i, e$, and d are of the general form $K_\alpha = g_\alpha W_\alpha$, where $g_\alpha = V_\alpha/\Lambda^3 q_{\text{inter},\alpha}$. $W_\alpha = \exp[\beta(\mu - E_\alpha)]$. To obtain μ of the CO_2 molecule in the bulk: ideal gas. Contribution of vibrations are important at relevant pressures and temperatures.

Model-experiment

- This leads to $K_\alpha = r_q \beta P V_\alpha e^{-\beta E_\alpha}$
- Even for non-zero K_e , isotherm of adsorbed CO_2 as a function of pressure shows sharp step when $K_i > K_1, K_e$.
- For each metal, two comparisons are made:
- 2- Predictive mode: binding energies obtained from DFT calculations - left panel.
- 1- Binding energies taken from experiment - right panel.
- Mg and Mn: 1-lane model (transverse dimers negligible).
Others: 6-lane model.

Model-experiment

- This leads to $K_\alpha = r_q \beta P V_\alpha e^{-\beta E_\alpha}$
- Even for non-zero K_e , isotherm of adsorbed CO_2 as a function of pressure shows sharp step when $K_i > K_1, K_e$.
- For each metal, two comparisons are made:
- 2- Predictive mode: binding energies obtained from DFT calculations - left panel.
- 1- Binding energies taken from experiment - right panel.
- Mg and Mn: 1-lane model (transverse dimers negligible).
Others: 6-lane model.

Model-experiment

- This leads to $K_\alpha = r_q \beta P V_\alpha e^{-\beta E_\alpha}$
- Even for non-zero K_e , isotherm of adsorbed CO_2 as a function of pressure shows sharp step when $K_i > K_1, K_e$.
- For each metal, two comparisons are made:
 - 2- Predictive mode: binding energies obtained from DFT calculations - left panel.
 - 1- Binding energies taken from experiment - right panel.
- Mg and Mn: 1-lane model (transverse dimers negligible).
Others: 6-lane model.

Model-experiment

- This leads to $K_\alpha = r_q \beta P V_\alpha e^{-\beta E_\alpha}$
- Even for non-zero K_e , isotherm of adsorbed CO_2 as a function of pressure shows sharp step when $K_i > K_1, K_e$.
- For each metal, two comparisons are made:
- 2- Predictive mode: binding energies obtained from DFT calculations - left panel.
- 1- Binding energies taken from experiment - right panel.
- Mg and Mn: 1-lane model (transverse dimers negligible).
Others: 6-lane model.

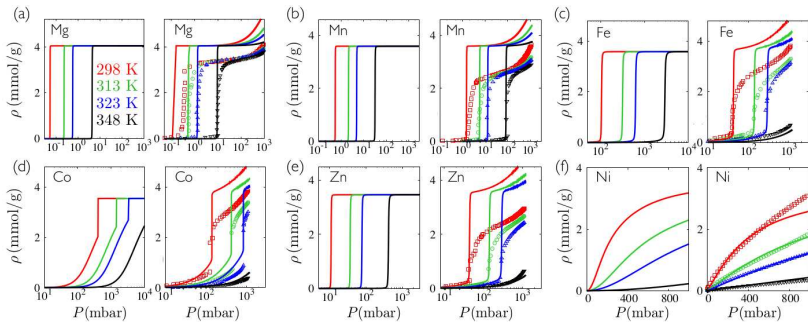
Model-experiment

- This leads to $K_\alpha = r_q \beta P V_\alpha e^{-\beta E_\alpha}$
- Even for non-zero K_e , isotherm of adsorbed CO_2 as a function of pressure shows sharp step when $K_i > K_1, K_e$.
- For each metal, two comparisons are made:
- 2- Predictive mode: binding energies obtained from DFT calculations - left panel.
- 1- Binding energies taken from experiment - right panel.
- Mg and Mn: 1-lane model (transverse dimers negligible).
Others: 6-lane model.

Model-experiment

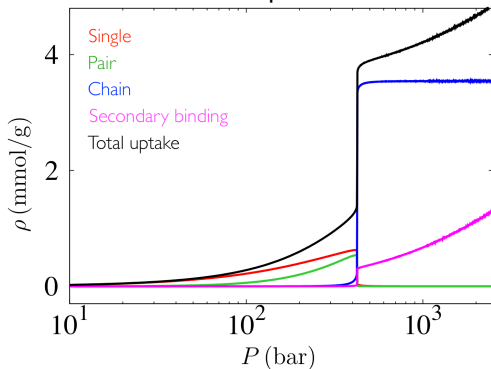
- This leads to $K_\alpha = r_q \beta P V_\alpha e^{-\beta E_\alpha}$
- Even for non-zero K_e , isotherm of adsorbed CO_2 as a function of pressure shows sharp step when $K_i > K_1, K_e$.
- For each metal, two comparisons are made:
- 2- Predictive mode: binding energies obtained from DFT calculations - left panel.
- 1- Binding energies taken from experiment - right panel.
- Mg and Mn: 1-lane model (transverse dimers negligible).
Others: 6-lane model.

Data



Refinements

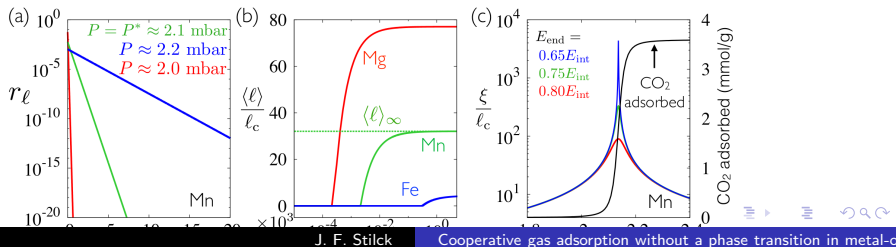
Fine features (rising of isotherm before the step and after the step):
introduce secondary binding sites where monomers may adsorb.
Densities of different types of adsorbed monomers may be
accessible to NMR experiments. Results for Mn, 6-lane model:



Chain length distribution and correlation length

The (exponential) chain length distribution $r_\ell \times \ell$ may be found in the 1-lane model (J. F. Stilck, M. A. Neto, and W. G. Dantas, Physica A **368**, 442 (2006)). Use site dependent statistical weights K_i .

Bond-bond correlation length ξ ($\langle \eta_i \eta_{i+\ell} \rangle - \langle \eta_i \rangle^2 \approx e^{-\ell/\xi}$), in units of lattice spacing may also be obtained (Pfeuty & Wheeler) ($\xi = 1/\ln(\lambda_1/\lambda_2)$). Results (a,c): Mn at 313 K. (b) Different metals at 313 K.



Conclusion

- No phase transition necessary to explain abrupt rise in isotherm of MOF.
- Model provides understanding for reasons of features of isotherms. Example: increasing K_i/K_e leads to more abrupt isotherms.
- May suggest how to induce cooperativity by introducing additional binding agents.
- Model with quenched defects may be relevant to compare data in many cases, work in this direction is being done.

Conclusion

- No phase transition necessary to explain abrupt rise in isotherm of MOF.
- Model provides understanding for reasons of features of isotherms. Example: increasing K_i/K_e leads to more abrupt isotherms.
- May suggest how to induce cooperativity by introducing additional binding agents.
- Model with quenched defects may be relevant to compare data in many cases, work in this direction is being done.

Conclusion

- No phase transition necessary to explain abrupt rise in isotherm of MOF.
- Model provides understanding for reasons of features of isotherms. Example: increasing K_i/K_e leads to more abrupt isotherms.
- May suggest how to induce cooperativity by introducing additional binding agents.
- Model with quenched defects may be relevant to compare data in many cases, work in this direction is being done.

Conclusion

- No phase transition necessary to explain abrupt rise in isotherm of MOF.
- Model provides understanding for reasons of features of isotherms. Example: increasing K_i/K_e leads to more abrupt isotherms.
- May suggest how to induce cooperativity by introducing additional binding agents.
- Model with quenched defects may be relevant to compare data in many cases, work in this direction is being done.